Research Article

Journal of PeptideScience

Received: 6 April 2010 Revised: 10 August 2010 Accepted: 12 August 2010 Published online in Wiley Online Library: 20 September 2010

(wileyonlinelibrary.com) DOI 10.1002/psc.1297

Synthesis and conformational analysis of salivary proline-rich peptide P-B

Elżbieta Kamysz* and Emilia Sikorska

The 57-amino acid human salivary polypeptide P-B has been synthesized by the solid-phase method using 9-fluorenylmethoxycarbonyl (Fmoc) strategy. The circular dichroism (CD) spectroscopy, Fourier-transform infrared spectroscopy (FTIR) and molecular modeling methods have been used for conformational studies of P-B. Examination of the CD spectra of P-B showed the content of the secondary structure to be independent of temperature over the range 0–60 °C at pH = 7 as well as over the pH range of 2–12 at 37 °C. P-B adopts predominantly unordered structure with locally appearing β-turns. The cumulative results obtained using the CD and FTIR spectroscopic techniques indicate the percentage of the polyproline type-II (PPII) helix being as low as about 10%. Similarly, the molecular dynamics (MD) simulations reveal only a short PPII helix in the *C*-terminal fragment of the peptide (Pro^{51}–Pro^{54}), which constitutes 7%. Copyright © 2010 European Peptide Society and John Wiley & Sons, Ltd.

Keywords: salivary proline-rich proteins; peptide synthesis; CD spectroscopy; Fourier-transform infrared spectroscopy; molecular modeling

Introduction

The salivary proline-rich proteins (PRPs) predominate in the human saliva and constitute up to 70% of the proteins secreted by the parotid gland [1]. PRPs have commonly been classified into three categories: acidic, basic and glycosylated proteins. Acidic PRPs bind to the surface of teeth and are involved in calcium and hydroxyapatite homeostasis and dental pellicle formation [2]. Glycosylated PRPs bind and agglutinate oral bacteria and have lubricating properties [3]. Basic PRPs bind and precipitate polyphenols by forming insoluble complexes, so that they can pass harmlessly through the body [4,5]. The high affinity of PRPs for polyphenols has been attributed to their open and extended structure and their high proline content. Recently, an unidentified basic PRP has been shown to inhibit HIV-1 infectivity [6]. To date, the function of this category of human salivary protein has not been well established.

The most common conformation of the proline-rich sequences is the polyproline type-II (PPII) helix, a left-handed helix consisting of *trans*-prolines with backbone dihedrals $\phi = -75^{\circ}$ and $\psi = +145^{\circ}$, resulting in a very extended structure with a highly solvated backbone and three residues per turn [7,8]. Results of conformational studies of PRPs suggested the occurrence of the poly-L-proline form II conformation. However, there are still some discrepancies in the interpretation of conformations of this line of peptides in solution [9–11].

In this paper, we report the results of chemical synthesis and conformational studies of P–B, a member of the basic proline-rich protein family present in the human saliva. It is a 57-amino acid peptide containing 30 proline and 9 glycine residues, pQRGPRGPYPPG-PLAPPQPFGPGFVPPPPPPPYGPGRIPPPPPAPYGPGIFPPPPPQP. The P-B is a mature peptide by itself [12–15], but its biological role remains still unclear [16,17]. Previous circular dichroism (CD) studies of P–B, based on the coincidence of the positions of trough and peak in the CD spectrum of the aqueous solution of poly-L-proline with that of P–B, indicated that the consecutive prolyl residues in the peptide adopt a poly-L-proline form II structure [18]. However, it is known that among all protein residues adopting PPII dihedral angles, only about 50% constitute part of PPII helices of four residues or longer and the CD spectra corresponding to the PPII fraction, obtained by both considering PPII segments and all the isolated residues in PPII conformational state, display identical characteristics of the poly(Pro)II helix bands [7,19,20]. For this reason, it is difficult to demonstrate the occurrence of the PPII conformation by CD alone. Hence, in our studies, apart from the CD spectroscopy, we have included Fourier-transform infrared spectroscopy (FTIR) and molecular modeling to determine the conformational properties of the P-B peptide.

Materials and Methods

Peptide Synthesis

The [Q^1]P-B peptide was synthesized manually by the solid-phase method on a 2-chlorotrityl chloride resin (loading 1.3 mmol/g, 1% DVB, 100–200 mesh, Tianjin Nankai Hecheng Science & Technology Co., Ltd., China) using 9-fluorenylmethoxycarbonyl (Fmoc) chemistry [21]. *N*-α-Fmoc-protected amino acids were purchased from Iris Biotech GmbH (Germany); 1-hydroxybenzotriazole (HOBt), piperidine, diisopropylocarbodiimide (DIC)

* *Correspondence to: Elżbieta Kamysz, University of Gdańsk, Sobieskiego 18, 80-952 Gdańsk, Poland. E-mail: kamysz@chem.univ.gda.pl*

University of Gdańsk, Sobieskiego 18, 80-952 Gdańsk, Poland

Abbreviations used: *ACN, acetonitrile; DCM, dichloromethane; DIC, diisopropylocarbodiimide; DIEA, N,N-diisopropylethylamine; DMF, N,N-dimethylformamide; HOBt, 1-hydroxybenzotriazole; Pbf, 2,2,4,6,7-pentamethyldihydrobenzofurane-5-sulfonyl; pQ, pyroglutamic acid; PRP, proline-rich protein; TBTU, O-(benzotriazol-1-yl)-1,1,3,3-tetramethyluronium tetrafluoroborate; tBu, t-butyl; TFA, trifluoroacetic acid; Trt, trityl.*

and chloranil were from Fluka (Switzerland); *N*,*N*-diisopropylethylamine (DIEA), triisopropylsilane, *O*-(benzotriazol-1-yl)-1,1,3,3-tetramethyluronium tetrafluoroborate (TBTU) and phenol were from Sigma-Aldrich (Poland); acetonitrile, *N*,*N*-dimethylformamide (DMF), dichloromethane (DCM), diethyl ether and acetic acid were from Polish Chemicals (Poland).

The *N*-α-Fmoc-amino acids were protected on the side chain as follows: trityl (Trt) for glutamine, *t*-butyl (tBu) for tyrosine, and 2,2,4,6,7-pentamethyldihydrobenzofurane-5-sulfonyl (Pbf) for arginine. The attachment of the first amino acid to the resin was performed according to Barlos *et al*. with a loading of 0.6 mmol/g [22]. Deprotection of the Fmoc group was carried out for 10 and 20 min with 25% piperidine in DMF. All amino acids were coupled with a fivefold molar excess of the protected amino acid (Fmoc-AA) dissolved in DMF/DCM using HOBt and DIC for 2–5 h (Fmoc-AA : HOBt : DIC, 1 : 1 : 1). Only the coupling reactions of Fmoc-Gln(Trt)-OH were carried out using also TBTU with the addition of HOBt in the presence of DIEA for 2 h (Fmoc-AA : TBTU : HOBt : DIEA, 1 : 1 : 1 : 2). The completeness of each coupling step was monitored by the chloranil test.

Cleavage of the Peptide from the Resin

After the synthesis had been completed, the final peptide [Q^1]P-B was cleaved from the resin and the protecting groups removed with a trifluoroacetic acid (TFA)/triisopropylsilane/water/phenol (94 : 2.5 : 2.5 : 1 v/v/v/v) mixture for 2 h. The cleaved peptide was precipitated with cold diethyl ether and lyophilized.

Purification and Analysis

The crude [Q^1]P-B peptide obtained in this way was purified by reversed-phase high performance liquid chromatography (RP-HPLC) on a Kromasil C8 column (8 $\times$ 250 mm, 5 µm particle size) with several linear gradients of acetonitrile (ACN) in 0.1% TFA. The eluates were fractionated and analyzed by analytical RP-HPLC. The purity of the peptide was checked on an analytical Beckman chromatograph with a Kromasil C8 column (4.6 $\times$ 250 mm, 5 µm particle size) with several linear gradients of ACN in 0.1% TFA. Fractions containing the pure peptide (>98%) were pooled and lyophilized. The ([Q^1]P-B) peptide was then analyzed by matrix-assisted laser desorption ionization-time of flight mass spectrometry (MALDI-TOF MS) and electrospray ionization mass spectrometry (ESI-MS). The value of the molecular ion was as expected.

P-B was obtained from [Q^1]P-B. The cyclization reaction of the *N*-terminal Gln residue was conducted in acetic acid solution at room temperature. The progress of the reaction was monitored by RP-HPLC. After completing the cyclization, acetic acid was evaporated and the residue was dissolved in water and lyophilized. The obtained P-B peptide was purified by RP-HPLC as described and analyzed by MALDI-TOF MS and ESI-MS.

Mass Spectrometry

The MALDI-TOF MS spectral analysis was performed on the Bruker Biflex III MALDI-TOF mass spectrometer using an ultraviolet laser source (nitrogen, 337 nm). α-Cyano-4-hydroxycinnamic acid was used as a spectrometric matrix.

The ESI-MS spectral analysis was performed on a Bruker microTOF-Q mass spectrometer. Samples of the peptides were dissolved in an acetonitrile/water (1 : 1; v/v) mixture containing 0.1% formic acid and infused by a syringe pump with a flow rate of 3 µl/min. The instrument was operated in a positive mode over the range 500–3000 *m/z*.

Peptide [Q^1]P-B: MALDI-TOF MS: m/z = 5806.07 (M^+, calc), m/z = 5807 ($[MH]^+$, found). ESI-MS: m/z = 5806.07 (M^+, calc), m/z = 1162.21 ($[M+5H]^{5+}$, calc), m/z = 1162.8 ($[M+5H]^{5+}$, found), m/z = 1452.52 ($[M+4H]^{4+}$, calc), m/z = 1453.5 ($[M+4H]^{4+}$, found), m/z = 1936.36 ($[M+3H]^{3+}$, calc), m/z = 1937.4 ($[M+3H]^{3+}$, found).

Peptide P-B: MALDI-TOF MS: m/z = 5789.03 (M^+, calc), m/z = 5790 ($[MH]^+$, found). ESI-MS: m/z = 5789.03 (M^+, calc), m/z = 1158.81 ($[M+5H]^{5+}$, calc), m/z = 1159.4 ($[M+5H]^{5+}$, found), m/z = 1448.26 ($[M+4H]^{4+}$, calc), m/z = 1449.0 ($[M+4H]^{4+}$, found), m/z = 1930.68 ($[M+3H]^{3+}$, calc), m/z = 1932.0 ($[M+3H]^{3+}$, found).

CD Measurements

CD spectra were recorded on a P-B sample in a Britton–Robinson buffer (a mixture of 0.04 M H_3BO_3, 0.04 M H_3PO_4 and 0.04 M CH_3COOH) that has been adjusted to the desired pH (2, 5, 7, 10 and 12) by titration with a 0.2 M NaOH solution), at 37 °C. In addition, the CD spectra were recorded at pH = 7 over the temperature range of 0–60 °C at each 5 °C interval.

The measurements were conducted on 0.1 mM peptide solutions. A Jasco J-85 spectropolarimeter with a 2 cm/min scan speed was used (Physicochemical Laboratories, Faculty of Chemistry, University of Gdansk, Poland). Although the spectra were recorded over the 190–240 nm range, their fragments below ~195 nm were not always reliable due to strong interferences of the solvent at those wavelengths. The CD spectra were measured in triplicate and plotted as mean ellipticity Θ (degree $\times$ cm^2 $\times$ $dmol^{-1}$) *versus* wavelength λ (nm). The content of the secondary structure was calculated from the spectra using a CONTINLL method [23].

FTIR Measurements

The spectra were recorded at 25 °C as average of 16 scans with the spectral resolution of 4 cm^{-1} using a model IFS66 Bruker infrared spectrometer equipped with a mid-infrared Globar light source and a DT–GS detector (Physicochemical Laboratories, Faculty of Chemistry, University of Gdansk, Poland). A sample was deuterated by the incubation of the peptide in deuterated water and then lyophilized. Completeness of the proton–deuterium exchange was confirmed by the disappearance of the amide II band corresponding to the N–H bending vibrational mode. The samples in the hydrated film were prepared by dissolving the peptide in deuterated water (2% w/v), placing 10 µl of the solution on to the CaF_2 window and evaporating the solvent with nitrogen gas to form a thin hydrated film. Spectral processing was carried out and analyzed using the Grams/32 program from Galactic (Galactic Industries Co., Salem, NH). All the spectra were analyzed by both deconvolution and second derivative methods [24,25] to determine the number and positions of peaks assignable to the amide I′ band. Deconvolution of the spectra was done over the range 1800–1500 cm^{-1} using a gamma factor of 3.0. A nine-point Savitzky–Golay smoothing function was applied to calculate the second derivative. The initial linewidths were set to 10 cm^{-1}. The deconvoluted spectra were fitted to Gaussian band profiles. The quality of the fitting was estimated by standard deviation.

Journal of PeptideScience

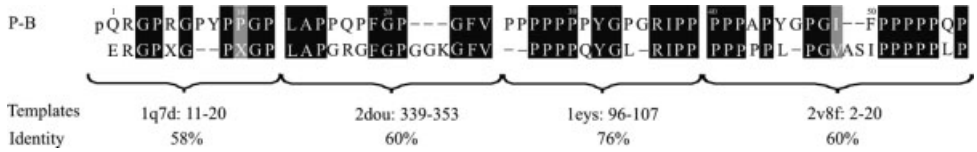

Figure 1. Alignment of sequences of templates, 1q7d: 11–20; 2dou: 339–353; 1eys: 96–107 and 2v8f: 2–20 with sequence of P-B for homology modeling of a chimera protein P–B. The identical residues are shown in black, while those with similar properties are shown in gray. Symbol X corresponds to 4-hydroxyproline.

Molecular Modeling

A non-standard residue, pyroglutamic acid (pQ), was parameterized as recommended in the AMBER 8.0 manual [26]. Specifically, it was modeled using bond lengths, valence and torsion angles of a compatible molecular segment from the Cambridge Structural Database (CSD) [27]. The atomic charges for pQ were optimized by fitting them to the *ab initio* molecular electrostatic potential, obtained from GAMESS [28] in the 6-31G* base, for two different conformations, followed by consecutive averaging of the charges over all conformations, as recommended by the RESP [29] module.

A poor homology over the entire range of sequence and the absence of a template protein poses problems for homology modeling of P–B. The problem was overcome by building a chimera model, based on the coordinates of fragments of four different proteins (1q7d: 11–20; 2dou: 339–353; 1eys: 96–107 and 2v8f: 2–20) found in the Protein Data Bank, using BLASTP 2.2.22 [30]. The sequential homology between appropriate fragments of P-B and their homolog structures is about 60% (Figure 1). Subsequently, suitable computer mutations of the structures were performed using a SwissPBDViewer [31] program. Specifically, the residues were replaced from the templates with equivalent ones from P-B essentially on a one-to-one basis (for specific residue substitutions, see sequence alignment in Figure 1). Finally, the entire P-B model was energy-minimized to remove unfavorable steric clashes. Since, all the X-Pro peptide bonds in the template structures were *trans*, the geometry of all the peptide groups in P-B model were kept fixed in *trans* configuration with $f = 50$ kcal/(mol $\times$ rad^2) during the entire simulation.

The initial solvent configuration around the peptide was obtained by filling a cubic box with water molecules. The overall box size was enlarged by about 10 Å in each direction. A total number of 4421 water molecules were used. The chloride ions were used to neutralize the entire system. To equilibrate the solution's density, the entire assembly was subjected to NPT dynamics, at a pressure of 1 atm, at 298 K, for 1 ns, with positional constraints on all Cα atoms. Next, the entire system was submitted to the molecular dynamics (MD) simulations in a periodic box of constant volume. The positional proline Cα constraints were used exclusively for 4 ns of the NVT simulations. In further NVT simulations (8 ns), the positional Cα constraints were removed. The total duration of the run was 13 ns. The time step was 2 fs. The MD simulations were carried out using a particle-mesh Ewald (PME) procedure [32]. The coordinates were collected every 2000th step. The last 50 conformations were considered in further analysis.

The results obtained were analyzed using the Carnal and Ptraj programs from the AMBER 8.0 package [26]. The molecular structures were drawn and analyzed with the graphic programs VMD [33] and MOLMOL [34].

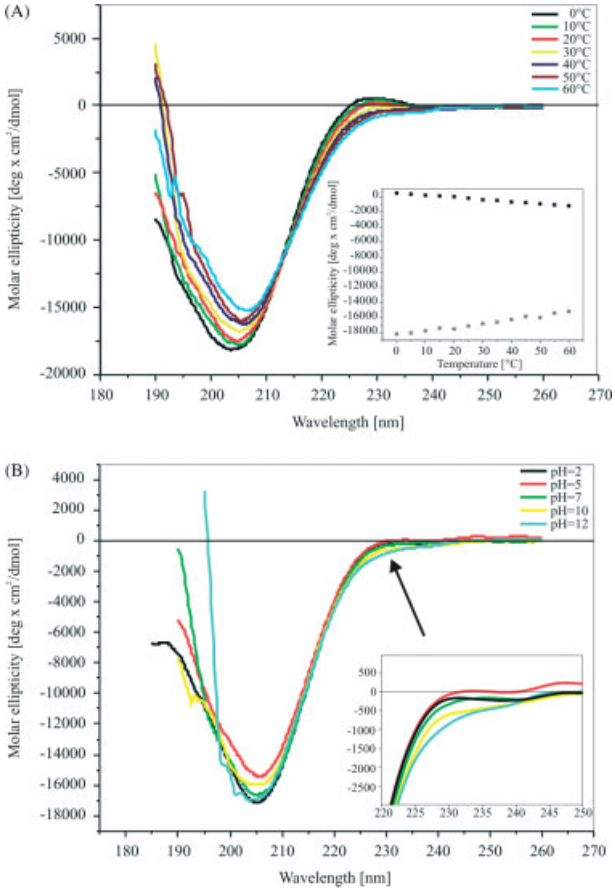

Figure 2. CD spectra of P-B in the Britton–Robinson buffer (A) at pH = 7, over the temperature range of 0–60 °C. Inset: temperature dependence of the molar ellipticities at 206 nm (gray square) and 228 (black square) and (B) in the Britton–Robinson buffers of different pH's, at 37 °C.

Results and Discussion

Circular Dichroism (CD)

The CD spectra of P-B as a function of temperature are shown in Figure 2. As seen, their characteristic feature is the presence of a deep and broad negative maximum at ~206 nm and a positive shoulder at ~228 nm, which can be assigned to a poly(Pro)II helix [35]. Isodichroic point around 213 nm suggests the existence of an equilibrium of unordered and PPII conformations. The intensities of both negative and positive bands decreased gradually upon raising the temperature (inset of Figure 2(A)), but the PPII structure was still present at 60 °C. A progressive reduction and a slight red shift of the bands around 213 and 228 nm upon increase in temperature may be indicative of the presence of β-turns, being favored at elevated temperature [36]. However, a quantitative analysis of the CD spectra (Table 1) clearly indicates that there are

Table 1. The percentage of different secondary motifs in P-B calculated on the basis of CD spectra at different temperatures

T (°C)	α-helix (%)	β-strand (%)	Turns (%)	PPII (%)	Unordered (%)
0	5	10	16	12	57
5	5	27	16	12	40
10	5	23	16	11	45
15	6	29	17	12	36
20	5	18	17	10	50
25	6	29	16	11	38
30	5	26	18	12	39
35	6	18	14	8	54
40	6	24	17	12	41
45	5	19	17	10	49
50	7	26	18	11	38
55	6	21	16	9	48
60	6	19	16	9	50

Table 2. The percentage of different secondary motifs in P-B calculated on the basis of CD spectra at different pH's

pH	α-helix (%)	β-strand (%)	Turns (%)	PPII (%)	Unordered (%)
2	5	9	16	10	60
5	5	18	17	10	50
7	6	24	18	11	41
10	5	10	14	8	63
12	7	22	19	12	40

no large conformational changes over that temperature range and a noticeable growth of β-turn contribution is not observed. The P-B assumes predominantly a statistical-coil conformation with locally appearing β-turns, whereas PPII constitutes only about 10% of the peptide structure. As shown, the P-B does not possess a well-ordered structure; however, strong steric interactions between prolyl rings [37] make it difficult for a complete denaturation of the peptide.

It is known that the differences in conformational behavior could be related to the change of the overall peptide charge. As the peptide charge is dependent on both the external pH and pK_a values of the functional groups, P-B has also been investigated by measuring the CD as a function of pH (Figure 2) to estimate electrostatic contribution to the structure. The CD spectra were recorded within a pH range of 2–12. The overall charge of P-B is equal to +2 and −1 over the ranges of 2–10 and 10–12, respectively. The spectra recorded over the broad pH range are very similar (Table 2). The spectra taken at extremal pH's, 2 and 12, showed only a small increase in the intensity at 206 nm (~3%) as compared to the spectrum at neutral pH. In turn, increasing the pH to 12, which is well above the pK_a of 10.13 for the hydroxyl group of tyrosine [38] results in a considerable loss in the intensity of the 228 nm band. This finding suggests the tyrosine side-chain contribution to the 228 nm band [39]. Nevertheless, the lack of substantial pH effects shows that ionic interactions are only minor determinants of the P-B structure.

Fourier-transform Infrared Spectroscopy (FTIR)

To further analyze the conformational properties of P–B, FTIR spectroscopy was employed. As a structural probe, an amide

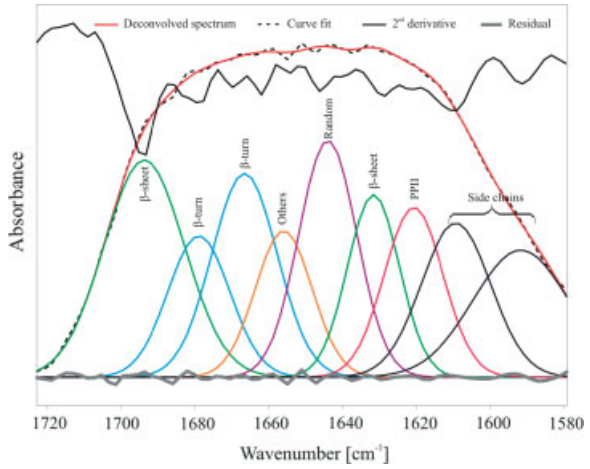

Figure 3. Fourier-deconvoluted amide I′ band of hydrated P-B, fitted with a sum of Gaussian bands. The reduced χ of this fit was 1.84, with a correlation coefficient of >0.99.

Table 3. Positions, linewidths and relative areas of the bands over the range 1720–1580 cm^{-1} fitted to the Fourier deconvoluted spectra of P-B

Position (cm^{-1})	Structural element	Width (cm^{-1})	Real area (%)
1694	β-sheet	26	17
1679	β-turn	20	9
1666	β-turn	20	13
1656	Others: α-helix, PPII, extended turn structure and/or statistical-coil	18	8
1644	Random	18	13
1632	β-sheet or extended structure	16	9
1621	Hydrated PPII	19	10
1609	Side-chain vibrations	22	10
1592		30	10

I′ band was used to represent primarily the C=O stretching vibration of the amide groups [40]. P-B in the hydrated film exhibits a broad amide I′ band with a maximum at 1643 cm^{-1}. Deconvolution and derivation of the band enabled to distinguish individual components and to assign each of them a specific conformational type (Figure 3; Table 3) [41]. The analysis revealed nine major peaks at 1694, 1679, 1666, 1656, 1644, 1632, 1621, 1609 and 1592 cm^{-1} in the 1720–1580 cm^{-1} range. However, the last two correspond to side-chain vibrations. Bands in the regions of 1640–1620 and 1690–1700 cm^{-1} have been assigned to β-sheet components [25,42]. Nevertheless, it should be noticed that the β-sheet's low-frequency band (1632 cm^{-1}) might arise from vibrations of short extended segments that do not form β-sheet [43]. In turn, two peaks at 1666 and 1679 cm^{-1} can be attributed to β-turns [44], whereas a broad peak at 1644 cm^{-1} was assigned to the statistical-coil structure [24,25].

The absorbance peak at 1656 cm^{-1} is usually assigned to α-helix, but because ~70% of the total number of P-B amino acids are Pro and Gly, which are strong α-helix breakers, it is highly unlikely that this protein contains a lot of helical structures. Furthermore, the CD results indicate the presence of very few α-domains (~6%).

Journal of PeptideScience

Table 4. The percentage of different structural motifs in P-B calculated on the basis of deconvoluted FTIR spectra in the hydrated film

Structural motif	Content (%)
β-sheet	33
Turns	27
Random	18
PPII	12
Others	10

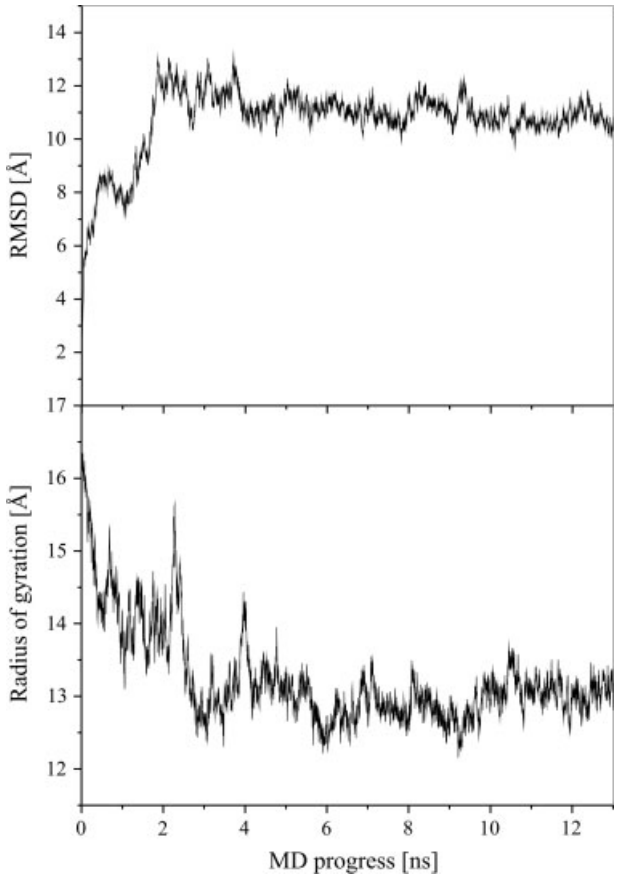

Figure 4. RMSD and radius of gyration (R_g) values along the trajectory from the initial structure.

Hence, the 1656 cm^{-1} absorbance band can be assigned to a statistical-coil with some impact of Gln side-chain absorbance, as was suggested for PRPI [45]. In turn, Dukor and Keiderling [46] reported that peaks at 1656 and 1620 cm^{-1} in D_2O could be displayed by short runs of poly-L-proline (3–6 residues). Therefore, the 1656 cm^{-1} band together with the 1621 cm^{-1} one in the FTIR spectrum of P-B is likely to indicate a PPII helix conformation. However, as far as the unambiguous assignment of the 1656 cm^{-1} band seems vague, the 1621 cm^{-1} one can definitely be attributed to the hydrated PPII helix [45].

The different structural motifs in the peptide, calculated on the basis of the deconvoluted FTIR spectra, are collected in Table 4.

Figure 5. Superimposition of the last 50 structures of P-B obtained during 13 ns of the MD simulations. $RMSD_{5-12} = 1.052$ Å for backbone atoms, respectively. Blue color marks turn structures, white – unordered and cyan – polyproline II (PPII).

Molecular Modeling

Figure 4 shows the RMSD computed for the backbone atoms relative to the starting point of the simulations. The RMSD plot indicates that the P-B changes its conformation for the first 4 ns of MD simulations and then maintains that conformation up to the end of the simulations. In turn, inspection of the radii of gyration (R_g) as a function of time (Figure 4) shows that the global shape of the backbone changes considerably during the first 6 ns of simulations and the P-B conformation becomes more compact as compared to that at the starting point. Afterward, the R_g values fluctuate around an equilibrium value, which indicates that the overall conformation of P-B remains unchanged. The radius of gyration averaged for the last 50 conformations amounts to 13.1 Å, which is $<$15.7 Å for an initial conformation of P-B. The last 50 structures of P-B are shown in Figure 5.

A Ramachandran map of the conformational states of each amino acid residue of the last 50 P-B conformations is presented in Figure 6(A). It can be seen that the conformational states of all individual P-B residues (ϕ, ψ) pairs are grouped into two clusters, which correspond to PPII states and the type I and III β-turns states. However, the analysis of the angle distribution plots (Figure 6(B)) revealed that although 30% of the individual amino acid residues of the conformational ensemble are found in the region of conformational space characteristic of PPII, only 7% are a part of PPII helices (fragment Pro^{51}–Pro–Pro–Pro^{54}). The rest of the peptide is unordered with locally appearing β-turns. Nevertheless, no proline *cis* $\leftrightarrow$ *trans* isomerization were included in simulations. It should be emphasized that the consideration of the *cis*–*trans* isomerization could decrease the PPII percentage. On the other hand, the lower content of PPII would be incompatible with the experimental data.

To bind plant polyphenols from the diet, the proline residues should be exposed to create a highly accessible binding site for them. It is possible when the proline residues are involved in the PPII helix formation. However, besides the PPII helix, the statistical-coil, turns and β-strands are the most readily accessible folds, with an average of 30% of accessible surface [47]. In the case of P-B, more than a half of the amino acids, therein 50% comprising proline residues, possess at least 30% of their relative surface accessible (Figure 7). Moreover, the proline residues are compacted to form a large hydrophobic surface that can readily

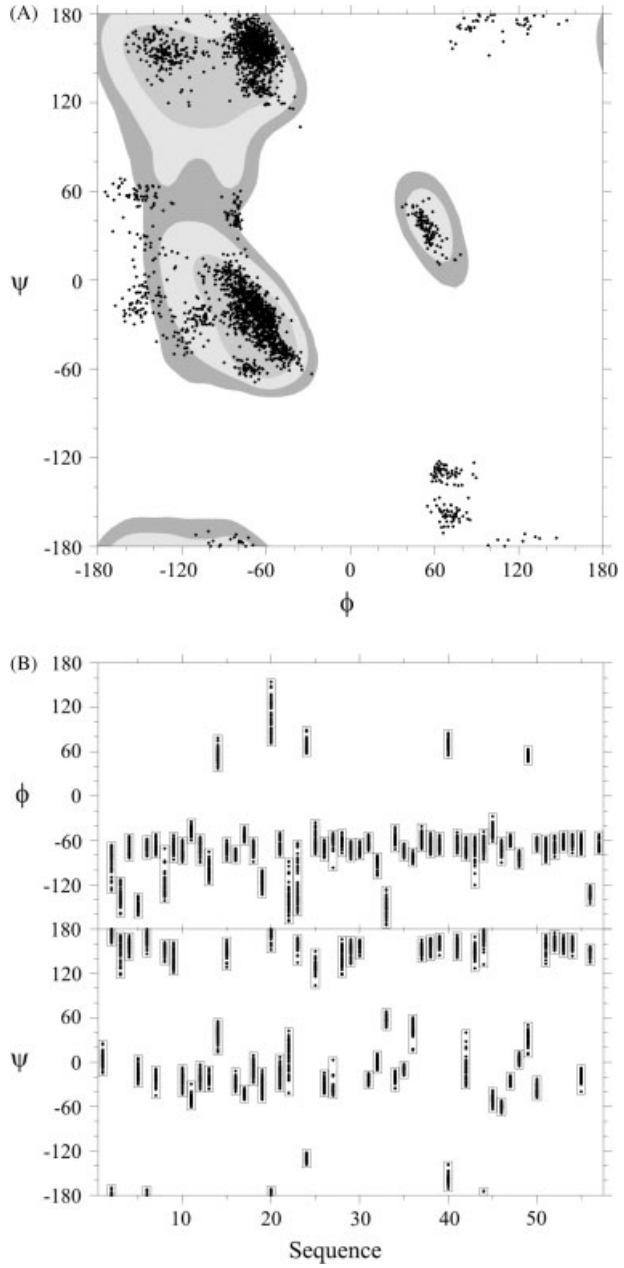

Figure 6. Ramachandran plot of the dihedral angles (ϕ and ψ) (A) and angle distribution bars (ϕ and ψ) (B) of all residues of the last 50 conformations of P-B obtained during 13 ns of the MD simulations.

bind to other hydrophobic surfaces such as aromatic rings of polyphenols (Figure 8).

Conclusions

To the best of our knowledge, the chemically synthesized entire proline-rich human protein has recently been reported only for the basic PRP IB7 peptide [11], whereas the synthesis of P-B is now reported for the first time.

The cumulative results obtained using the CD and FTIR spectroscopic techniques have shown that the P-B conformation presents predominantly a mixture of an unordered and β-turn structures. In turn, the content of the PPII helix does not exceed

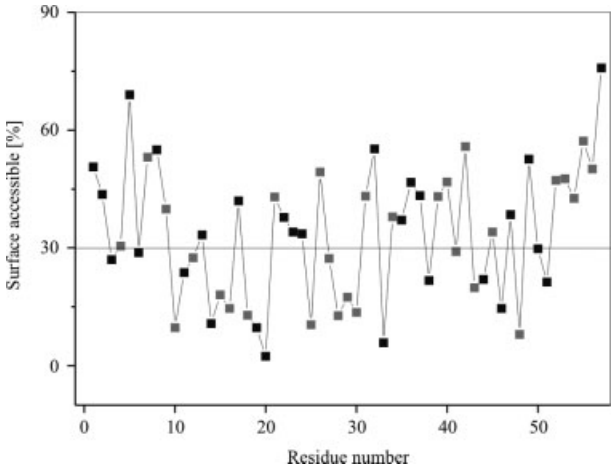

Figure 7. The average surface accessibility of amino acid residues of P-B calculated for the last 50 conformations obtained during 13 ns of the MD simulations. Gray squares denote Pro residues.

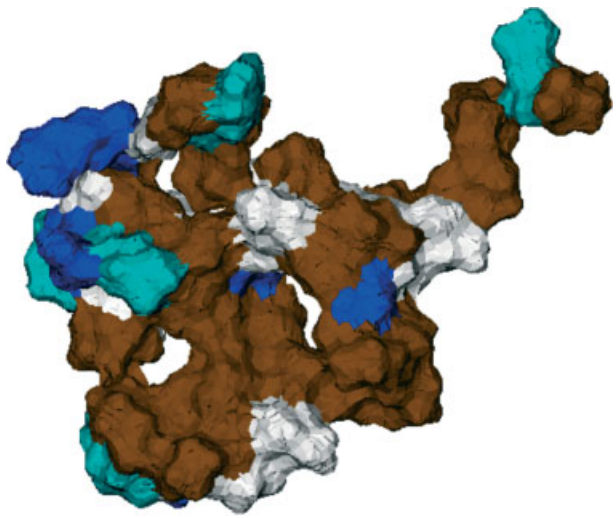

Figure 8. Molecular surface of the final structure of P-B colored by residue type. Ocher marks the Pro residue; white nonpolar residues (except for Pro); blue positively charged residues, whereas cyan polar, uncharged residues.

12%. Similarly, the MD simulations reveal the existence of only a short PPII helix in the *C*-terminal fragment of the peptide (Pro^{51}–Pro^{54}), which constitutes 7% of the peptide structure. In addition, the CD spectra clearly indicate that the P-B conformation is not influenced by thermal treatment and it is practically independent of the pH over the range of 2–12.

Acknowledgements

We are grateful to Prof. Szewczuk of the University of Wrocław for performing ESI-MS spectra and providing valuable remarks. This work was supported by the University of Gdańsk (DS 8452-4-0135-0, DS 8360-4-0133-0 and BW 8000-5-0254-9).

References

1 Kauffman DL, Keller PJ. The basic proline-rich proteins in human parotid saliva from a single subject. *Arch. Oral Biol.* 1979; **24**: 249–256.

2 Bennick A. Salivary proline-rich proteins. *Mol. Cell Biochem.* 1982; **45**: 83–99.
3 Bergey EJ, Levine MJ, Reddy MS, Bradway SD, Al-Hashimi I. Use of the photoaffinity cross-linking agent N-hydroxysuccinimidyl-4-azidosalicylic acid to characterize salivary-glycoprotein-bacterial interactions. *J. Biochem.* 1986; **234**: 43–48.
4 Lu Y, Bennick A. Interaction of tannin with human salivary proline-rich proteins. *Arch. Oral Biol.* 1998; **43**: 717–728.
5 Charlton AJ, Baxter NJ, Lilley H, Haslam E, McDonald Ch J, Williamson MP. Tannin interactions with a full-length human salivary proline-rich protein display a stronger affinity than with single proline-rich repeats. *FEBS Lett.* 1996; **382**: 289–292.
6 Robinovitch MR, Ashley RL, Iversen JM, Vigoren EM, Oppenheim FG, Lamkin M. Parotid salivary basic proline-rich proteins inhibit HIV-I infectivity. *Oral Dis.* 2001; **7**: 86–93.
7 Adzhubei AA, Sternberg MJE. Left-handed polyproline II helices commonly occur in globular proteins. *J. Mol. Biol.* 1993; **229**: 472–493.
8 Zhong H, Carlson HA. Conformational studies of polyprolines. *J. Chem. Theory Comput.* 2006; **2**: 342–353.
9 Shibata S, Asakura J, Isemura T, Isemura S, Saitoh E, Sanada K. Conformational study of the basic proline-rich polypeptides from human parotid saliva. *Int. J. Peptide Protein Res.* 1984; **23**: 158–165.
10 Murray NJ, Williamson MP. Conformational study of a salivary proline-rich protein repeat sequence. *Eur. J. Biochem.* 1994; **219**: 915–921.
11 Simon C, Pianet I, Dufourc EJ. Synthesis and circular dichroism study of the human salivary proline-rich protein IB7. *J. Pept. Sci.* 2003; **9**: 125–131.
12 Isemura S, Saitoh E. Molecular cloning and sequence analysis of cDNA coding for the precursor of the human salivary proline-rich peptide P-B. *J. Biochem.* 1994; **115**: 1101–1106.
13 Isemura S, Saitoh E. Nucleotide sequence of Gene PBI encoding a protein homologous to salivary proline-rich protein P-B. *J. Biochem.* 1997; **121**: 1025–1030.
14 Isemura S. Nucleotide sequence of gene PBII encoding salivary proline-rich protein P-B. *J. Biochem.* 2000; **127**: 393–398.
15 Isemura S, Watanabe S, Fujiwara S, Sanada K. Tissue distribution and nucleotide sequence of bovine mRNA for salivary proline-rich protein P-B. *Arch. Oral Biol.* 2004; **49**: 881–887.
16 Ayad M, Van Wuyckhuyse BC, Minaguchi K, Raubertas RF, Bedi GS, Billings RJ, Bowen WH, Tabak LA. The association of basic proline-rich peptides from human parotid gland secretions with caries experience. *J. Dent. Res.* 2000; **79**: 976–982.
17 Inzitari R, Cabras T, Rossetti DV, Fanali Ch, Vitali A, Pellegrini M, Paludetti G, Manni A, Giardina B, Messana I, Castagnola M. Detection in human saliva of different statherin and P-B fragments and derivatives. *Proteomics* 2006; **6**: 6370–6379.
18 Isemura T, Asakura S, Shibata S, Isemura S, Saitoh E, Sanada K. Conformational study of the salivary proline-rich polypeptides. *Int. J. Peptide Protein Res.* 1983; **21**: 281–287.
19 Stapley BJ, Creamer TP. A survey of left-handed polyproline II helices. *Protein Sci.* 1999; **8**: 587–595.
20 Sreerama N, Woody RW. Poly(Pro)II helices in globular proteins: identification and circular dichroism analysis. *Biochemistry* 1994; **33**: 10022–10025.
21 Chan WC, White PD. *Fmoc Solid Phase Peptide Synthesis. A Practical Approach*. Oxford University Press: Oxford, 2000.
22 Barlos K, Chatzi O, Gatos D, Stavropoulos G. 2-Chlorotrityl chloride resin. Studies on anchoring of Fmoc-amino acids and peptide cleavage. *Int. J. Pept. Protein Res.* 1991; **37**: 513–520.
23 Sreerama N, Woody RW. Estimation of protein secondary structure from circular dichroism spectra: comparison of CONTIN, SELCON, and CDSSTR methods with an expanded reference set. *Anal. Biochem.* 2000; **287**: 252–260.
24 Surewicz WK, Mantsch HH. New insight into protein secondary structure from resolution-enhanced infrared spectra. *Biochim. Biophys. Acta* 1988; **952**: 115–130.
25 Byler DM, Susi H. Examination of the secondary structure of proteins by deconvolved FTIR spectra. *Biopolymers* 1986; **25**: 469–487.
26 Case DA, Darden TA, Cheatham TE III, Simmerling CL, Wang J, Duke RE, Luo R, Merz KM, Wang B, Pearlman DA, Crowley M, Brozell S, Tsui V, Gohlke H, Mongan J, Hornak V, Cui G, Beroza P, Schafmeister C, Caldwell JW, Ross WS, Kollman PA. *AMBER 8*, University of California: San Francisco, 2004.
27 Allen FH. The Cambridge structural database: a quarter of a million crystal structures and rising. *Acta Crystallogr.* 2002; **B58**: 380–388.
28 Schmidt MW, Baldridge KK, Boatz JA, Elbert ST, Gordon MS, Jensen JH, Koseki S, Matsunaga N, Nguyen KA, Su S, Windus TL, Dupuis M, Montgomery JA. General atomic and molecular electronic structure system. *J. Comput. Chem.* 1993; **14**: 1347–1363.
29 Bayly CL, Cieplak P, Cornell WD, Kollman PA. A well-behaved electrostatic potential based method using charge restraints for deriving atomic charges: The RESP model. *J. Phys. Chem.* 1993; **97**: 10269–10280.
30 Altschul SF, Madden TL, Schäffer AA, Zhang J, Zhang Z, Miller W, Lipman DJ. Gapped BLAST and PSI-BLAST: a new generation of protein database search programs. *Nucleic Acids Res.* 1997; **25**: 3389–3402.
31 Guex N, Peitsch MC. SWISS-MODEL and the Swiss-PdbViewer: an environment for comparative protein modeling. *Electrophoresis* 1997; **18**: 2714–2723.
32 Darden T, York D, Petersen L. Partial mesh ewald: an N x log(N) method for ewalds sums in large systems. *J. Chem. Phys.* 1993; **98**: 10089–10092.
33 Humphrey W, Dalke A, Schulten K. VMD – visual molecular dynamics. *J. Mol. Graphics* 1996; **14**: 33–38.
34 Koradi R, Billeter M, Wüthrich K. MOLMOL: a program for display and analysis of macromolecular structures. *J. Mol. Graphics* 1996; **14**: 52–55.
35 Woody RW. Circular dichroism and conformation of unordered polypeptides. *Adv. Biophys. Chem.* 1992; **2**: 37–79.
36 Bochicchio B, Pepe A, Tamburro AM. Investigating by CD the molecular mechanism of elasticity of elastomeric proteins. *Chirality* 2008; **20**: 985–994.
37 Creamer TP. Left-handed polyproline II helix formation is (very) locally driven. *Proteins* 1998; **33**: 218–226.
38 Dawson RMC, Elliott DC, Elliott WH, Jones KM (eds). *Data for Biochemical Research*, Oxford University Press: New York, 1969.
39 Haas W, MacColl R, Banas JA. Circular dichroism analysis of the glucan domain of Streptococcus mutans glucan binding protein-A. *Biochim. Biophys. Acta* 1998; **1384**: 112–120.
40 Kong J, Shaoning Y. Fourier transform infrared spectroscopic analysis of protein secondary structures. *Acta Biochim. Biophys. Sinica* 2007; **39**: 549–559.
41 Venyaminov SY, Kalnin NN. Quantitative IR spectrophotometry of peptide compounds in water (H_2O) solutions. I. Spectral parameters of amino acid residue absorption bands. *Biopolymers* 1990; **30**: 1243–1257.
42 Vass E, Hollósi M, Besson F, Buchet R. Vibrational spectroscopic detection of beta- and gamma-turns in synthetic and natural peptides and proteins. *Chem. Rev.* 2003; **103**: 1917–1954.
43 Haris PI, Severcan F. FTIR spectroscopic characterization of protein structure in aqueous and non-aqueous media. *J. Mol. Cat. B* 1999; **7**: 207–221.
44 Dong A, Huang P, Caughey WS. Protein secondary structures in water from the second derivative amide I infrared spectra. *Biochemistry* 1990; **29**: 3303–3308.
45 Elangovan S, Margolis HC, Oppenheim FG, Beniash E. Conformational changes in salivary proline-rich protein 1 upon adsorption to calcium phosphate crystals. *Langmuir* 2007; **23**: 11200–11205.
46 Dukor RK, Keiderling TA. Reassessment of the random coil conformation: vibrational CD study of proline oligopeptides and related polypeptides. *Biopolymers* 1991; **31**: 1747–1761.
47 Lins L, Thomas A, Brasseur R. Analysis of accessible surface of residues in proteins. *Protein Sci.* 2003; **12**: 1406–1417.

